Defense Technical Information Center Compilation Part Notice

This paper is a part of the following report:

- *Title:* Technology Showcase: Integrated Monitoring, Diagnostics and Failure Prevention. Proceedings of a Joint Conference, Mobile, Alabama, April 22-26, 1996.

- *To order the complete compilation report, use:* AD-A325 558

The component part is provided here to allow users access to individually authored sections of proceedings, annals, symposia, etc. However, the component should be considered within the context of the overall compilation report and not as a stand-alone technical report.

SYNC-PERIOD FREQUENCY ANALYSIS AND ITS APPLICATION TO THE DIAGNOSIS OF MULTIPLE ELEMENT DEFECTS OF ROLLING BEARINGS

Wen-Yi Wang Michael J. Harrap

Acoustics and Vibration Center
Department of Aerospace and Mechanical Engineering
University College of UNSW
Australian Defence Force Academy
Campbell, ACT 2600
Australia

Abstract: A method for diagnosing multiple element defects of rolling bearings has been investigated. The method combines the time synchronous averaging and envelope spectral analysis techniques to produce spectra of synchronously averaged envelope signals with a range of synchronous frequencies. The spectra are displayed in the domains of synchronous period versus frequency to result in the sync-period frequency distribution. The distribution separates the characteristic defect frequencies and their associated sidebands in the synchronous period axis. This analysis technique makes it possible to detect and diagnose multiple defects appearing on different elements of rolling bearings. Another main benefit of the method is the significant noise reduction by both enveloping and synchronous averaging process. Analysis results from computer simulated data and experimental simulated data are presented.

Key Words: Defects diagnosis; Multiple defects; Rolling bearings; Synchronous average; Sync-period frequency analy s; Vibration analysis.

1. Introduction

Time synchronous averaging is a powerful tool to extract periodic waveforms from noisy signals. It has been used extensively in diagnosing gear defects. However, this technique has not found wide acceptance for diagnosing defects of rolling bearings, because of the asynchronous rotation [1] between the shaft and the rolling elements or cage of the rolling bearing, and the approximation of bearing characteristic defect frequencies [2]. On the other hand, the high frequency resonance technique (HFRT) is widely accepted in bearing defect diagnosis. For single defect cases, it has proven successful under reasonable signal to noise ratio (*SNR*) conditions, provided that the shaft is running at a constant speed and there exists no skidding of the rolling elements. But this

technique has proven less than satisfactory in detecting bearing defects under poor *SNR* conditions [3]. Also, to the authors knowledge, the successful application of this technique to the diagnosis of multiple element defects in bearings has not been reported.

In diagnosing multiple faults, Igarashi and Kato [4] investigated the vibration of a ball bearing with multiple defects on the race surface of **either the inner or outer ring** under given thrust loads. Using an FFT analyzer and examining the effect of the measuring position of the outer ring on the vibration, they clarified the fundamental characteristics of ball bearings with multiple faults, and they also established an approach to locate the faults and indicate the number and size of the defects. Mcfadden and Smith [5] described an investigation of a bearing with multiple point defects based on their model [6] of a single point defect. The vibration envelope spectra produced by a bearing with **multiple inner race defects** were illustrated by the reinforcement and cancellation of spectral lines due to the different phase angle of the vibrations induced by different faults. Braun and Datner [7] discussed a bearing fault diagnostic method based on time averaging. The RMS level of the averaged signal was utilized to indicate the relevant defects according to their characteristic defect frequencies. This method effectively extracts the periodic signals associated with bearing faults from noisy structural vibrations and is less sensitive to structure parameters than general spectral techniques. However, the RMS approach seems not capable of identifying which frequency components contribute the most to the RMS value, because one averaging period could involve several frequency components. Moreover, due to the low energy of the vibration caused by bearing faults, the characteristic defect frequencies may be very difficult to be discerned when the shaft rotation related frequency components (high energy) are closely adjacent to those defect frequencies.

The high frequency resonance technique is effective in excluding the shaft rotation related frequency components, but it has no advantage in separating multiple defect frequencies and eliminating high frequency noise disturbances. In cases where bearings have multiple defects located in different elements, each defect may have different shape and size. Thus each defect may excite a different resonance (structural and/or transducer's) to a different extent. Using the ordinary high frequency resonance technique, only one resonance is isolated by a bandpass filter for envelope detection. Therefore, where multiple faults exist, multiple defect frequency components are likely to be mixed together, provided all defects excite the same resonance to a comparable extent. Alternatively, if a particular resonance is dominated by one fault excitation, then only that fault will be distinguishable.

In this paper, we investigate a technique which introduces an averaging process into the high frequency resonance technique and expands the bandwidth of the bandpass (or even high pass) filter to include several high frequency resonances rather than just a single isolated resonance. The time synchronous averaging process is performed after the envelope detection. Due to the uncertainty of the bearing's characteristic defect frequencies, the synchronous frequency is swept around the nominal defect frequency until the true frequency is identified. Spectral analysis is then carried out for the resulting averaged envelope signal. The spectra are finally displayed in the so-called *syncperiod - frequency domain* to form the *syncperiod - frequency (SPF) distribution*. In SPF distributions, the individual characteristic defect frequencies and their associated modulation sidebands are well separated along the syncperiod axis. The exact frequency content

can then be acquired so as to diagnose the condition of the bearing with multiple element defects. It is shown that the enveloping and synchronous averaging processes used in this method significantly improve the signal to noise ratio.

2. Sync-Period Frequency (SPF) Analysis

In this section, a method which combines the time synchronous averaging technique and the high frequency resonance technique is described. From the high frequency resonance technique, we know that the envelope signal generated by localized bearing defects can be featured as a series of exponentially decayed impulses with the periods related to various defects [6, 7]. For the remaining part of this section, we are only dealing with the envelope signals.

2.1. Time Synchronous Averaging of a Bearing Signal and Its Spectrum

Using standard envelope detector, the raw signal is firstly bandpass filtered in the high frequency resonance region. The resulting signal consists of the bearing defect induced signal embedded in band-limited Gaussian noise. Suppose $x(t)$ is such an envelope signal, and it contains frequency components corresponding to the harmonics of the characteristic defect frequencies and their associated sidebands. It is decomposed into N segments, each of same length T_s. Each segment is separated by a variable period τ ($\tau \geq T_s$ – ie. no overlap). Summing up all these segments yields:

$$y(t,\tau) = \sum_{n=0}^{N-1} x(t+n\tau), \qquad t \in [0, T_s] \tag{1}$$

where τ is the averaging period, T_s is the segment length. According to the time-shift theorem of Fourier transform, the spectrum of (1) $Y(f,\tau)$ will be [8,9]

$$Y(f,\tau) = X(f) \cdot \sum_{n=0}^{N-1} e^{j2\pi fn\tau} = X(f) \cdot \frac{\sin N\pi f\tau}{\sin \pi f\tau} \cdot e^{j(N-1)\pi f\tau} \tag{2}$$

the amplitude spectrum will then yield

$$|Y(f,\tau)| = |X(f)| \cdot \left| \frac{\sin N\pi f\tau}{\sin \pi f\tau} \right| \tag{3}$$

which is the original amplitude spectrum $|X(f)|$ multiplied by the transfer function of a comb filter $|H(f)| = |\sin(N\pi f\tau)/\sin(\pi f\tau)|$. By examining the nature of the function $|H(f)|$ shown in Figure 1 [8, 9], we can see that **a)** it is a periodic function with the period of $f = 1/\tau$; **b)** for large N the function appears like a train of sinc functions and it becomes an impulse train when N goes to infinity, with period $f = 1/\tau$; **c)** its main lobes peak amplitude is N, they are located at $f = n/\tau$ ($n=0, 1, \ldots, N-1$), its first zero is at $f = 1/N\tau$ and thus the main lobes have the width of $B=2/N\tau$; **d)** its main lobe $3dB$ point is at $0.45/N\tau$, and thus $3dB$ bandwidth is $B_{3dB} = 0.9/N\tau$; **e)** its side lobe peaks decrease with increasing N, the maximum side lobe peak is $12dB$ down from the main lobe peak when $N=5$, and $13dB$ down when $N=20$, it approaches the limit value of $-13.3dB$ as N increases.

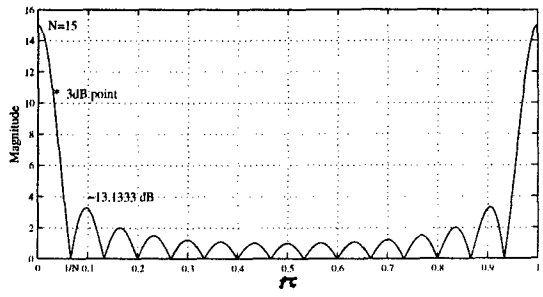

Figure 1. One period of function $|\sin(N\pi f\tau)/\sin(\pi f\tau)|$ [9]

As we mentioned early, $|X(f)|$ has the frequency components of mf_o, $mf_i \pm kf_r$, $mf_b \pm kf_c$ (m,k=0,1, 2,...) where f_o, f_i, f_b denote the characteristic defect frequencies of outer race, inner race and ball/roller respectively, f_r denotes shaft rotation frequency, f_c cage frequency. The relative amplitude of these components depend upon the damping factor of the bearing system, the load distribution and the variation of transmission path [1]. When the synchronous period τ equals an integer multiple M of the interval corresponding to one of the above frequencies, for instance $\tau=MT_o=M/f_o$, the frequency components from both signal and noise (except f_o and its harmonics) are rejected and a periodic signature with a period of T_o is extracted by the averaging process of (1) (see [10]). Therefore, the spectrum $|Y(f,\tau)|$ in (3) will be dominated by f_o and its harmonics.

2.2. Signal Processing Considerations

Due to the uncertainty of the characteristic defect frequencies of the bearings, it is necessary to identify the true synchronous period by searching around the nominal frequencies. The signal processing scheme that is used to find the true synchronous period is based on a search strategy (Figure 2).

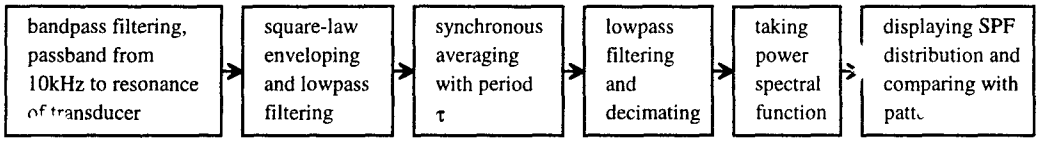

Figure 2. The flowchart of Sync-Period Frequency Analysis

In implementing the above scheme digitally, several factors have to be considered. In this section, we will discuss the effect of sampling rate f_s, data segment length T_s, synchronous period τ, the number of averages N and the search spacing $\Delta\tau$ on the performance of SPF analysis. For clarification, we tabulate all factors concerned in SPF analysis as following:

f_s	sampling frequency, $\Delta\tau_{min} = 1/f_s$
T	total data length
T_s	segmental data length
B	main lobes bandwidth of the comb filter, $B=2/N\tau$, $\Delta f \geqslant B$
B_{3dB}	main lobes 3dB bandwidth of the comb filter, $B_{3dB} = 0.9/N\tau$

f^*	defect frequency components to be detect
Δf	frequency accuracy, defined as $\Delta f = M[1/\tau - 1/(\tau+\Delta\tau)]$, $(\Delta f \simeq f\,\Delta\tau/\tau$, if $\Delta\tau << \tau)$
df	frequency resolution from the Fourier transform, $df = 1/T_s$
M	integer multiples of the defect periods
τ	synchronous period, $\tau = M/f^*$, $\tau \geqslant T_s$ (τ and T_s are in an equivalent order)
$\Delta\tau$	sync-period search spacing, $\Delta\tau/\tau = \Delta f/f^*$ (if $\Delta\tau << \tau$), $\Delta\tau \geqslant 1/f_s$
N	number of averages, N = mod (T, τ)

To ensure the correct detection of frequency components, we are particularly concerning about the search spacing $\Delta\tau$ with respect to the frequency accuracy Δf (frequency resolution obtained from the syncperiod). Large $\Delta\tau$ may fail to identify the bearing defect frequency, whereas too small $\Delta\tau$ may cause a tremendous increase of computing time. In general, $\Delta\tau$ is determined such that the frequency accuracy Δf is larger than (or equal to) the bandwidth [10] of comb filter's main lobes shown in Figure 1. According to the requirement of the SPF analysis, factors like f_s, f^*, $\Delta\tau$, Δf and B are primarily selected, and other factors are determined by the formula in the above table. Figure 3 depicts how non-dimensional measures $\Delta f/f^*$, $\Delta\tau/\tau$, $\Delta\tau f$, $\Delta f\tau$, $\Delta f/B$, N and M are related. The calculated factors could be verified by these non-dimensional graphs.

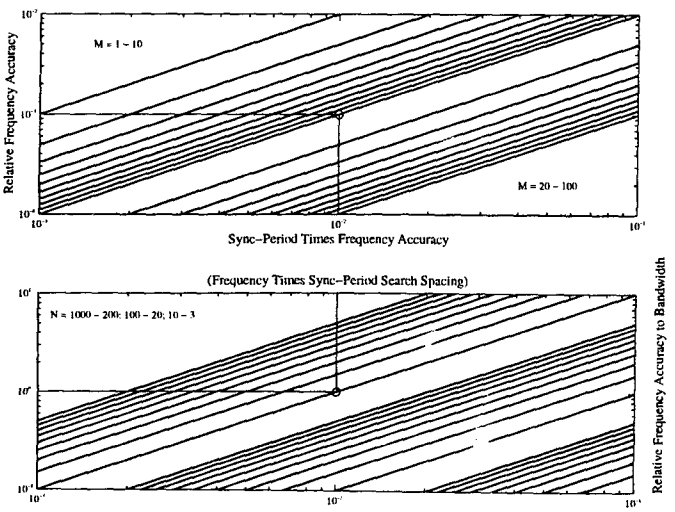

Figure 3. The relationship of $\Delta f/f^*$, $\Delta\tau/\tau$, $\Delta\tau f^*$, $\Delta f\tau$, $\Delta f/B$, N and M. (**a**) $\Delta f/f^*$ vs. $\Delta\tau f^*$ (or $\tau\Delta f$), both in logarithm scale, $\Delta f/f^* = \Delta\tau f^*/M$; (**b**) $\Delta f/B$ vs. $\Delta\tau f^*$ (or $\tau\Delta f$), both in logarithm scale, $\Delta f/B = \Delta\tau f^* N/2$.

For example, assuming the sampling rate is 100kHz which leads to a $\Delta\tau_{min}$ of 0.01ms, if we select $\Delta\tau$ = 0.04ms and Δf = 0.25Hz, then to detect a frequency component of 250Hz would require M to be 10, and τ to be 40ms. Furthermore, if we select $B = \Delta f$ = 0.25Hz, N would be 200 and T would be 8 s (800000 samples).

In detecting multiple frequency components, we need to sweep the synchronous period τ in a wide range. We can keep $\Delta\tau$ unchanged during the sweeping while using different M 's to associate with multiple f^* 's. In the above example, if there are three frequency components to be detected, eg. 152Hz, 198Hz, 247Hz, M's would be 4, 6 and 10 respectively, and the sweeping range of τ would be 26.32ms ~ 40.5ms. To ensure a successful search, the range could be expanded to 24ms ~ 43ms. If a fixed averaging number N (eg. 200) is selected, the frequency bandwidth B will vary from 0.42Hz to 0.23Hz, and Δf from 0.23Hz to 0.24Hz. Provided the range of $\Delta f/B$ is acceptable, fixed N is more convenient for sweeping. In this regard, the frequency resolution for low frequency components will be poorer due to the smaller $\Delta f/B$.

Following the averaging process, the frequency spectrum of the averaged envelope signal is estimated. The FFT associated frequency resolution of the spectrum df is therefore another concern. However, during sweep synchronous averaging the sync-period τ ($=M/f$) can give a much higher frequency resolution than what could be achieved through spectral analysis. The required df should be high enough to allow individual frequency components to be distinguished. For the above example, the spectral resolution df is about 38Hz ~ 25Hz ($1/\tau$).

3. SPF Pattern of Multiple Bearing Defects

The SPF patterns provide a graphical exhibition of the frequency composition of a signal in the frequency-syncperiod domain. In this section, we present a SPF pattern for a combination of different types of element defects using nominal characteristic defects frequencies [7, 11] of a bearing. The main uncertainty in estimating the characteristic frequencies is the contact angle between rolling elements of the races, which is dependent on the type of bearing and loading conditions. Another source of uncertainty is the diameter variations of the balls.

In the cases where multiple defects in different bearing elements exist and/or the *SNR* is poor, envelope spectra [6] prove unsatisfactory for the identification of individual bearing defect frequency components. SPF patterns indicate where the characteristic defect frequencies and their sidebands are located in a two dimensional domain (notice that the relative intensity is not shown), referred here as *'syncperoid - frequency domain'*. Syncperiod axis represents the sweeping range for the synchronous period τ which is an integer multiple of the characteristic defect periods. the frequency axis is used to define the frequency contents corresponding to a given the syncperiod. In fact, with small $\Delta\tau$ the syncperiod τ contains much finer frequency resolution than frequency axis. However, without the frequency axis, the syncperiod along would not be able to distinguish which frequency components this period multiple ($\tau=M/f^*$) is associated with. For instance, a syncperiod of 24ms could be either 6 times 4ms (250Hz) or 4 times 6ms (166.67Hz).

Now we consider a rolling bearing (NSK EN202) with different types of defects and present the SPF pattern associated with a combination of various defects. This type of bearing is deliberately chosen for the near harmonics of various defect frequencies, ie. $3f_r$ and f_o, f_i-f_r and f_b, $2f_o$ and f_i +f_r etc. are closely adjacent, which makes the diagnosis of defects more complex. Dimensions and defect frequencies of the bearing are listed below. The SPF pattern is shown in Figure 4.

ball number	ball diameter	pitch diameter	contact angle	shaft speed f_r	outer race frequency f_o	inner race frequency f_i	ball frequency f_b	cage frequnecy f_c
8	6.54mm	27.5mm	0°	50Hz	152.47Hz	247.53Hz	198.52	19.06Hz

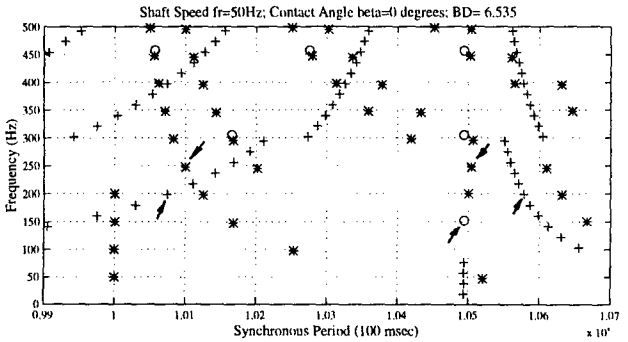

Figure 4. SPF pattern for a combination of outer race, inner race and roller/ball defects ('o' – outer race defect related components; '*' – inner race defect related components; '+' – ball/roller defect related components; all arrows are pointing at the fundamental defect frequencies)

4. Diagnosis of Multiple Defects Located in Different Bearing Elements Using SPF Analysis

In this section, we will discuss the application of the SPF analysis to detect multiple defects in different bearing elements. Results from both computer synthesised and experimental simulated data are described.

4.1. Diagnosis of Multiple Defects Generated by Models

The synthetic vibration signal used in this section is a bearing signal generated via Braun's model [2, 7] plus other vibration sources (eg. unbalanced shaft, etc.) and noise. The following example presents the SPF distribution from synthetic signal generated by the model. It consists of an impulse series induced by all three types of defects, shaft rotation related vibrations (narrow band but high power) and broadband white noise. The maximum impact amplitudes are 35, 90, 100 for the outer race defect, inner race defect and ball defects respectively. The noise standard deviation σ_n is 30. It is also assumed in our synthetic data that three different types of defects excite three different resonances, ie. f_1=25070Hz, f_2=18003Hz, f_3=21110Hz, and with different time constants of exponential decay, α_1=1/15, α_2=α_3=2/15, respectively. Using the SPF analysis described in section 2, the SPF distribution of the synthetic signal plus broadband white noise is generated and displayed in Figure 5. All factors used are tabulated below:

df	f_s	$\Delta f <$	$B <$	$T_s = \tau_{min}$	N	T	$\Delta\tau = \Delta\tau_{min}$	τ	M
10Hz	100kHz	0.03Hz	0.2Hz	100 ms	100	10.48576 s	0.01 ms	100.01~107 ms	16(f_o); 25,26(f_i); 20,21(f_b)

Comparing this SPF distribution with the SPF pattern shown in Figure 4, it is found that the characteristic defect frequency components and their associated modulation sidebands are well separated in syncperiod - frequency domain. For a given synchronous period, only one frequency component and its harmonics are exposed. It can be seen from the SPF distribution that the lower frequency components are more widely spreaded over the syncperiod domain. The noise level

has been significantly attenuated through enveloping (3dB improvement) [12] and averaging (a factor of $\sqrt{N}$) [10,13].

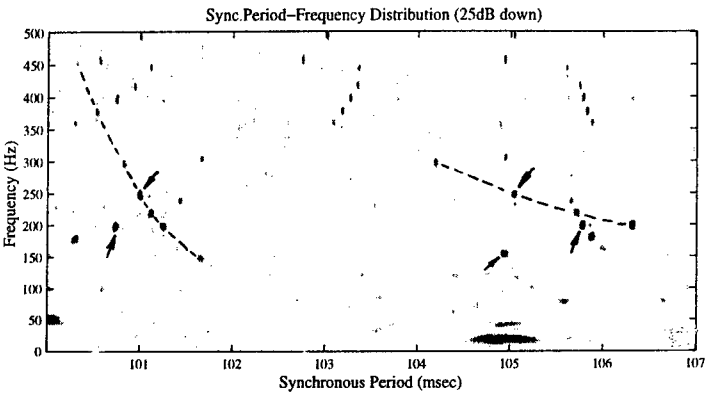

Figure 5. SPF distributions from synthetic signal plus broadband noise with σ_n=30

In fact, the original signal for Figure 5 has a very poor signal to noise ratio (-15.5 dB). From time domain, there is no evidence of any characteristic defect frequency related components because of high level noise disturbance and the intertwinement of multiple frequency components. Using the envelope spectral technique (Figure 6), it is also very difficult to identify individual characteristic defect frequencies.

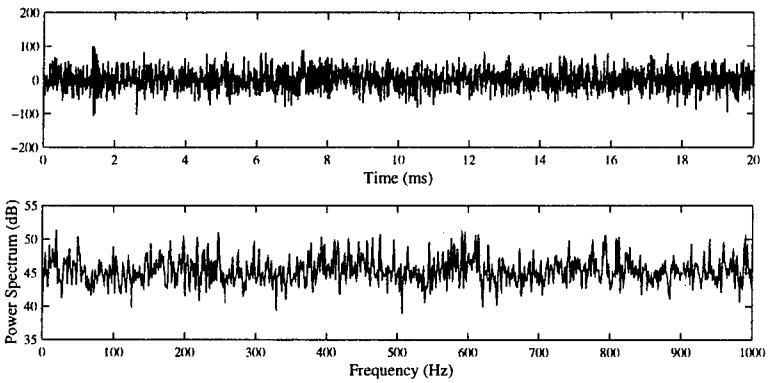

Figure 6. **(a)** Original time signal for Figure 5 and **(b)** the envelope spectrum (1024 averages) of (a)

4.2. Diagnosis of Multiple Defects With Experimental Data

Two NSK EN202 bearings were used for this experimental investigation. The artificial defects were implanted by either nitric acid corrosion or electric discharge erode. Bearing #1 has one defect on **both outer race and inner race** (nitric acid corrosion - about 2~3 mm in diameter, depth unknown but very shallow). Bearing #2 has one ball defect implanted (electric erode - diameter 0.38mm, depth 1mm), and its cage was dismantled and re-riveted after the introduction of the defect. The analysis results are shown in Figure 7 and 8. All SPF analysis parameters are identical to the examples in section 4.1 except the range of syncperiod τ for bearing #2 (from 99.01~107 ms). The experimental conditions are listed in the following table:

shaft speed	transducer	load applied	sampling rate	f_o, f_i, f_b, f_c
50 Hz	B&K 8307 (#1) B&K 4393 (#2)	240N radial (#1) 260N radial (#2)	100 kHz	152.47, 247.53, 198.52, 19.06 Hz (nominal defect frequencies)

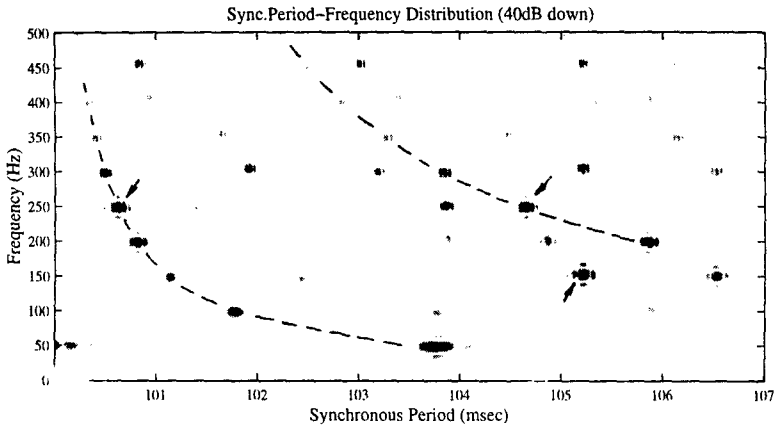

Figure 7. SPF distribution of Bearing #1, the signal was highpassed at 10kHz before enveloping.

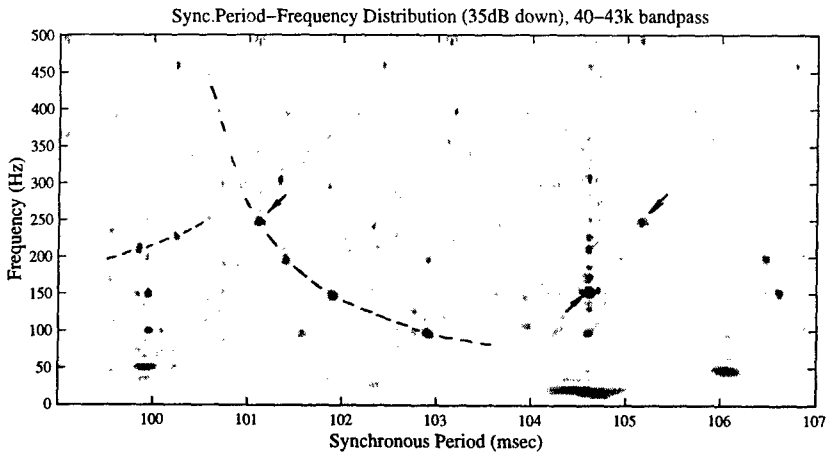

Figure 8. SPF distribution of Bearing #2, the signal was bandpassed at 40~43kHz before enveloping

5. Discussions and conclusion

By baseband spectrum analysis of vibration signal of bearing #1, it is found that a series of high frequency resonances have been excited. Envelope demodulated spectra at several resonances show both inner race and outer race defective frequencies and associated shaft rotation frequency, but all those frequency components are intertwined together. The SPF distribution shown in Figure 7 separates those frequencies along the syncperiod axis and shows the defective frequencies and the modulation sidebands explicitly. The outer race defect frequency is derived from the point at 105.23ms on syncperiod axis and about 150Hz on frequency axis, which corresponds to 152.05Hz (M is 16 here). The inner race defect frequency (248.43Hz, M is 25) is corresponding to the point at 100.63ms and 250Hz. The SPF distribution of bearing #2 displays a multiple defect pattern rather than a single ball defect pattern. The indication of inner race and

outer race defects are very strong. This curious phenomenon suggests that inner race and outer race defects may have been produced during dismantling and re-assembly of the bearing. The envelope spectrum from a low frequency resonance (2kHz ~ 4kHz) reveals inner race fault related components. The outer race defect frequency dominates the envelope spectrum demodulated about a 26k~28kHz resonance. Ball defect components could be seen from the envelope spectra of 2kHz highpassed and 17k~23kHz bandpassed signals. The SPF distribution from the 40~43kHz bandpassed signal seems to give the best presentation of all three types of defects. By inspecting Figure 8 closely, the ball defect frequency and its sidebands are only discernible with ease around 100msec region due to the small size of the defect. The cage component at around 104.65ms, which corresponds to 19.11Hz (M=2), is an important indication of ball damage.

In Figure 5,7,8, we notice that the low frequency components tend to spread over a wide syncperiod region. The reason for that may be explained by *uncertainty principle* [13]. Because the syncperiod domain is virtually a frequency scale, a certain length of data segment contains less cycles for low frequencies than those for high frequencies, which results in poorer frequency resolution.

The above discussion suggests that the syncperiod frequency analysis combines the benefits of both high frequency resonance technique and time synchronous averaging technique in overcoming problems like low-duty bearing related vibration and asynchronous rotation of rolling element bearings. It is therefore concluded that the syncperiod frequency analysis is potentially an effective method for the diagnostics of multiple defects presented in different bearing elements.

References

1.P.D. Mcfadden. "Condition Monitoring of Rolling Element Bearings by Vibration Analysis". Machine Condition Monitoring (Papers presented at a Seminar) 1990, p49-53. Mechanical Engineering Publications Limited for the Institution of Mechanical Engineers, London.

2.S. Braun. "The Signature Analysis of Sonic Bearing Vibrations". IEEE Transactions on Sonics and Ultrasonics SU-27 (5) 1980, p317-328.

3.W.Y. Wang and M.J. Harrap. "Fault Diagnosis of Ball Bearings Using Autocorrelation Technique". Proceedings of Vibration and Noise '95 (Venice, Italy), p36-44. Edited by M.J. Doogwin, Published by Staffordshire University.

4.T. Igarashi and H. Hamada. "Studies on the Vibration and Sound of Defective Rolling Bearings (Third Report: Vibration of Ball Bearings with Multiple Defect)". Bulletin of the JSME 28 (237) 1985, p492-499.

5.P.D. Mcfadden and J.D. Smith. "The Vibration Produced by Multiple Point Defects in a Rolling Element Bearing". Journal of Sound and Vibration 98, 1986, 263-273.

6.P.D. Mcfadden and J.D. Smith. "Model for the Vibration Produced by a Single Point Defect in a Rolling Element Bearing". Journal of Sound and Vibration 96, 1984, p69-82.

7.S. Braun and B. Datner. "Analysis of Roller/Ball Bearing Vibrations". Journal of Mechanical Design 101, 1979, p118-125.

8.W. L. Stutzman and G. A. Thiele. Antenna Theory and Design, pp124-133. New York: John Wiley & Sons, Inc. 1981.

9.W.S. Burdic. Radar Signal Analysis, pp92-128. Englewood Cliffs, N.J.: Prentice-Hall Inc. 1968.

10.S. Braun. "Extraction of Periodic Waveforms by Time Domain Averaging". Acustica 32, 1975, p69-77.

11.T.A. Harris Rolling Bearing Analysis, pp229-252. John Wiley & Sons. 1984.

12.J.A. Betts Signal Processing, Modulation and Noise, pp97-115. London: The English University Press Limited. 1971.

13.F.D. Coulon. Signal Theory and Processing, pp80-121,162-178. Dedham, M.A.: Artech House Inc. 1986.